

## Lobster eye X-ray optics: Data processing from two 1D modules

O. Nentvich, M. Urban, V. Stehlikova, L. Sieger and R. Hudec

*Czech Technical University in Prague, Faculty of Electrical Engineering  
Technicka 2, Prague 166 27, Czech Republic  
(E-mail: [ondrej.nentvich@fel.cvut.cz](mailto:ondrej.nentvich@fel.cvut.cz))*

Received: May 11, 2017; Accepted: July 4, 2017

**Abstract.** The X-ray imaging is usually done by Wolter I telescopes. They are suitable for imaging of a small part of the sky, not for all-sky monitoring. This monitoring could be done by a Lobster eye optics which can theoretically have a field of view up to 360 deg. All sky monitoring system enables a quick identification of source and its direction. This paper describes the possibility of using two independent one-dimensional Lobster Eye modules for this purpose instead of Wolter I and their post-processing into an 2D image. This arrangement allows scanning with less energy loss compared to Wolter I or two-dimensional Lobster Eye optics. It is most suitable especially for very weak sources.

**Key words:** Lobster eye optics – X-ray monitoring– Image processing – All-sky monitor

### 1. Introduction

Nowadays, Wolter I optics are used for astronomical imaging in X-ray spectrum (Wolter, 1952). There are several satellite missions with this type of optics. This optics has advantages such as the focus point but also disadvantages such as a small field of view (FOV), typically up to 1 deg. Chandra can be mentioned as an example of a telescope with FOV of 1 deg (Weisskopf et al., 2000) as well as proposed large X-ray mission Athena with 0.7 deg FOV (Barret et al., 2013). For this reason, telescopes equipped with Wolter I type optics are not suitable for all-sky monitoring.

Another type of X-ray optics is the Lobster Eye (LE) type. This kind of optics has a wider FOV compared to Wolter I type, theoretically up to 360 deg. This feature makes the Lobster Eye optics very suitable for all-sky monitoring (Hudec et al., 2015). The Lobster Eye optics can have several different configurations. The basic is an one-dimensional arrangement where the optical module has vertical or horizontal mirrors and each has its own detector. This method creates a line focus from the point source, which means that the 1D Lobster Eye optics cannot directly show real images. Another possible arrangement is a combination of two modules rotated perpendicularly to each other, it is called Angel's or Schmidt's arrangement (Angel, 1979; Schmidt, 1975). A combination of two

perpendicular LE modules allows getting a point focus from a point source of radiation.

A mathematical combination of two 1D images - taken perpendicularly to each other - can be reconstructed as a 2D image. Two independent 1D modules have lower losses than one 2D module because there is only single reflection. X-ray optics works on the reflection principle. Schmidt's, Angel's or Wolter's arrangement have two reflections, which causes greater attenuation of the beam, for example by shadowing, or undesirable scattering caused by surface micro-roughness. The one-dimensional Lobster Eye optics has only one reflection, so there is better gain and it is more suitable for less intensive sources.

## 2. Lobster eye optics

The Lobster eye optics works on the reflection principle as well as the Wolter I optics. There are two arrangements of LE optics, Angel's and Schmidt's arrangement (Angel, 1979; Schmidt, 1975). Illustration of the LE's principle is in Figure 1. The incoming beam is reflected under  $\theta$  angle to the focal point  $F$  and line focus is achieved while 1D optics is used.

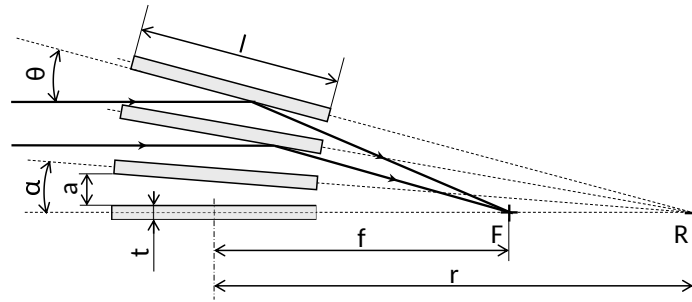


**Figure 1.** Schematic arrangement of a Lobster eye optics with incoming beam under  $\theta$  angle ( $t$  is mirror thickness,  $F$  is focus point,  $R$  is radius of curvature,  $l$  is length of mirror,  $a$  is distance between mirrors,  $\alpha$  is angle between two mirrors).

From Figure 1 it is possible to determine the direction of the source besides the radiation properties (spectrum, flux, ...). However, small changes need to be made for this determination.

A 1D Lobster eye optics produces a line focus and for evaluation of the direction of the X-ray source, it is necessary to determine a direction component i.e. a horizontal and a vertical part. The first component of the direction is determined by the position of the line focus in the image. The second direction component of the incoming beam is hard to identify without a hardware

improvement. It can be determined by placing a shading mask in front of the optics as shown in Figure 2. The shading mask produces gaps in the line focuses as is shown in Figure 3 and then it is possible to determine the second direction of the incoming beam. This improvement is included for example in the nanosatellite VZLUSAT-1, which carries 1D Lobster Eye module with this type of shading mask (Urban et al., 2016).

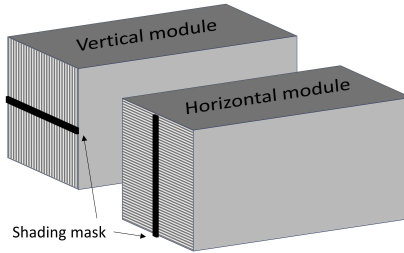


**Figure 2.** Illustration of the placement of shading masks for a horizontal and vertical module of Lobster eye optics

In the case of multiple sources in the FOV of the optics, the number of focal lines matches up with the number of sources. In Figure 3 there are line focuses for three point sources. Each source produces one line focus while 1D optics is used. In the left picture of Figure 3 there are only two line focuses, but in the bottom line, there are two gaps which belong to two point sources. Furthermore, it can be observed that the intensity of this line is higher than the intensity of the line produced only by one source.

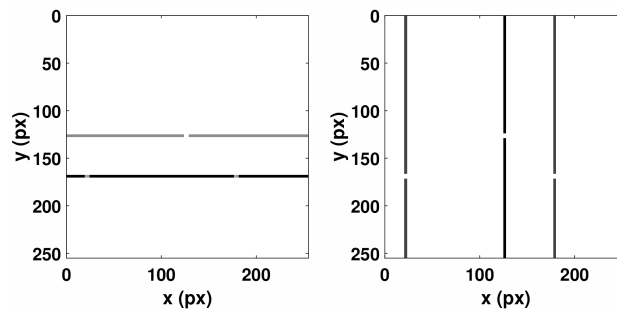


**Figure 3.** Line focuses for three point sources; the left image is for a horizontal LE optic module, the right image is for a vertical one

### 3. Image Reconstruction

The image reconstruction can be done by a matrix multiplication according to Equation 1 with the input images from Figure 3.

$$\mathbf{M} = \mathbf{H}\mathbf{V} \quad (1)$$

where  $\mathbf{M}$  is the result of matrix multiplication of the matrix  $\mathbf{H}$  corresponding to the horizontal and the matrix  $\mathbf{V}$  corresponding to the vertical input image. The images  $\mathbf{H}$  and  $\mathbf{V}$  have to be aligned according to the gaps in the line focuses.

This method is not useful for more than one line focus because the resulting image will contain  $n^2 - n$  imaginary sources ( $n$  is number of real point sources) as is shown in Figure 4. The matrix multiplication is extended by a Software (SW) mask for eliminating these imaginary sources and is based on the gaps in the line focuses which is introduced in the followings parts.

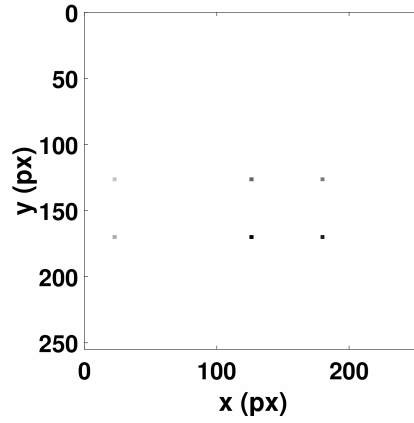


**Figure 4.** Resulting image based on three imaginary sources produced by matrix multiplication by Equation 1

#### 3.1. Software mask creation

The main goal of the SW mask is to eliminate imaginary sources in the final image. The SW mask  $\mathbf{I}$  is defined as described by Equation 2 and has the same resolution ( $x, y$ ) as the input images.

$$\mathbf{I}(x, y) = \begin{cases} 0, & \text{if } \mathbf{A}(x, y) > 0 \\ 1, & \text{otherwise} \end{cases} \quad (2)$$

The input matrix  $\mathbf{A}$  for  $\mathbf{I}$  is created as an element-wise multiplication of horizontal and vertical images as is described in Equation 3.

$$\mathbf{A} = \mathbf{H} \circ \mathbf{V} \quad (3)$$

The pixel's value at coordinates  $\mathbf{I}(x, y)$  is zero when the value  $\mathbf{A}(x, y)$  is greater than zero, otherwise it is one. However one more condition has to be met: gaps made by the shading mask must be in the same position in both vertical and horizontal images.

### 3.2. Final image

The resulting image  $\mathbf{R}$  is made according to Equation 4 as element-wise multiplication of SW mask  $\mathbf{I}$  and  $\mathbf{M}$ . This operation eliminates imaginary sources produced by matrix multiplication in the image  $\mathbf{M}$ .

$$\mathbf{R} = \mathbf{I} \circ \mathbf{M} \quad (4)$$

The final image based on Equation 4 is depicted in Figure 5 and contains only real point sources which are circled. Imaginary sources have been eliminated by SW mask  $\mathbf{I}$ . All equations were published in (Nentvich et al., 2017).

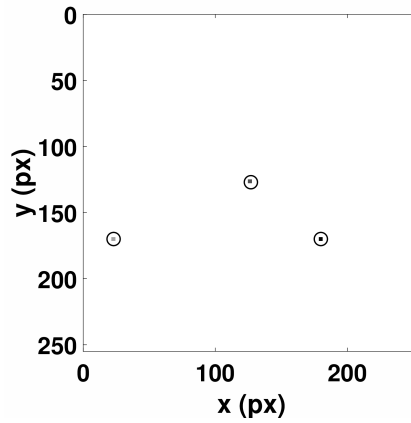


**Figure 5.** Image contains only real point sources which are circled

This algorithm can be applied, for example, on data downloaded from the nanosatellite VZLUSAT-1 which also carries the Lobster eye optics with a similar type of shading mask (Blazek et al., 2017; Pina et al., 2014; Urban et al., 2016).

## 4. Conclusion

This paper describes one of the first image reconstruction from two 1D Lobster eye optics. The algorithm now has some limitations – the gap in the line focuses has to be aligned in both pictures, because they are used for elimination of imaginary sources. Also, the noise is not presented in the images in this first approach. Otherwise, the SW mask should have unwanted holes caused by element-wise multiplication according to Equation 3 and then in the creation of the SW mask in Equation 2. It is necessary to improve the algorithm at least by a threshold.

This algorithm can be used for all sky monitoring on a satellite. The nanosatellite VZLUSAT-1 is equipped with one 1D Lobster eye optics and images downloaded from the VZLUSAT-1 can be processed using this algorithm.

**Acknowledgements.** This work was performed in cooperation with the company Rigaku Innovative Technologies Europe, s.r.o. It was supported by the Grant Agency of the Czech Technical University in Prague, grants No. SGS16/169/OHK3/2T/13 and SGS16/150/OHK3/2T/13 and by GA CR grant 13-33324S.

## References

- Angel, J. R. P. 1979, *Astrophys. J.*, **233**, 364
- Barret, D., Nandra, K., Barcons, X., et al. 2013, in SF2A-2013: Proceedings of the Annual meeting of the French Society of Astronomy and Astrophysics, ed. L. Cambresy, F. Martins, E. Nuss, & A. Palacios, 447–453
- Blazek, M., Pata, P., Inneman, A., & Skala, P. 2017, *Advances in Astronomy*, **2017**, 316289
- Hudec, R., Pina, L., Inneman, A., & Tichy, V. 2015, in SPIE Proceedings, Vol. 9510, EUV and X-ray Optics: Synergy between Laboratory and Space IV, 95100A
- Nentvich, O., Stehlikova, V., Urban, M., Hudec, R., & Sieger, L. 2017, in SPIE Proceedings, Vol. 10235, EUV and X-ray Optics: Synergy between Laboratory and Space
- Pina, L., Burrows, D., Cash, W., et al. 2014, in SPIE Proceedings, Vol. 9207, Advances in X-Ray/EUV Optics and Components IX, 92070T
- Schmidt, W. K. H. 1975, *Nuclear Instruments and Methods*, **127**, 285
- Urban, M., Nentvich, O., Stehlikova, V., et al. 2016, *submitted to Acta Astronautica*
- Weisskopf, M. C., Tananbaum, H. D., Van Speybroeck, L. P., & O’Dell, S. L. 2000, in SPIE Proceedings, Vol. 4012, X-Ray Optics, Instruments, and Missions III, ed. J. E. Truemper & B. Aschenbach, 2–16
- Wolter, H. 1952, *Annalen der Physik*, **445**, 94